Available online at www.sciencedirect.com
ScienceDirect
Journal of Photochemistry and Photobiology A: Chemistry 183 (2006) 190–197
Journal of Photochemistry and Photobiology A:Chemistry
www.elsevier.com/locate/jphotochem

Photophysical properties of an on/off fluorescent pH indicator excitable with visible light based on a borondipyrromethene-linked phenol

Wenwu Qin, Mukulesh Baruah, Wim M. De Borggraeve, Noël Boens *

Department of Chemistry, Katholieke Universiteit Leuven, Celestijnenlaan 200 F, 3001 Leuven, Belgium

Received 16 January 2006; received in revised form 10 March 2006; accepted 13 March 2006
Available online 28 March 2006

Abstract

A borondipyrromethene-derived pH indicator (available as methyl ester (**1**) and sodium salt (**2**)) for the near-neutral pH range with ultra bright fluorescence in the red spectral region has been synthesized by linking *o*-chlorophenol to the 3-position of a difluoroboradiazaindacene derivative. Absorption and steady-state and time-resolved fluorescence measurements have been used to study the photophysical properties of the BODIPY-based pH probe. The fluorescence lifetime (3.8 ± 0.2 ns) and the very high (nearly 1.0) fluorescence quantum yield of dye **1** are not dependent on the solvent. In aqueous solution, the water-soluble compound **2** undergoes a reversible protonation–deprotonation reaction in the near-neutral pH range with a pK_a of 7.60, which is practically insensitive to low ionic strength. Fluorimetric titrations as a function of pH produce fluorescence emission enhancements at lower pH.

Keywords: Fluorescent probe; PH sensor; Acidity constant; Borondipyrromethene; Spectroscopy

1. Introduction

Measurement of pH by fluorescence-based techniques is well established for both imaging and sensing applications [1]. Fluorescence offers significant advantages over other methods for physiological pH measurements due to its generally non-destructive character, high sensitivity and specificity, and the wide range of indicator dyes available [2]. Fluorescent pH indicators that can sense pH changes within the physiological range are an attractive target in molecular design and synthesis. Due to their excellent photophysical and optoelectronic properties, 4,4-difluoro-4-bora-3a,4a-diaza-*s*-indacene [3,4] (borondipyrromethene, BODIPY [5]) derivatives have become preferred fluorophores in new fluorescent probes that have applications in many different areas [6]. Some recent articles on BODIPY-based chemosensors describe probes for H^+ [7], Na^+ [8], K^+ [9], Ag^+ [10], and Zn^{2+} [11]. The valuable qualities of difluoroboradiaza-*s*-indacene fluorophores comprise relatively high absorption coefficients and fluorescence quantum yields (often approaching 1.0), narrow emission bandwidths with high peak intensities, elevated photostability and chemical stability, and excitation/emission wavelengths above 500 nm. Moreover, importantly, their spectroscopic properties can be fine-tuned by choosing appropriate substituents at the right positions.

Difluoroboradiaza-*s*-indacenes bearing hydroxyaryl subunits have been reported as pH indicators in aqueous-organic mixed media [12,13] and in aqueous solution [7]. The phenol derivatives [12] sense the alkaline pH range, while the calix[4]arene [13] and *o*-chlorophenol derivatives [7] are sensitive in the near-neutral pH range. The lack of fluorescence emission of the phenolate forms was attributed to an intramolecular charge transfer (ICT) between the phenolate anion and BODIPY subunits [7,12]. At lower pH a large fluorescence enhancement without spectral shift was observed.

Here, we report the synthesis and the pH dependent spectroscopic properties of *UBphen* – the methyl ester **1** and the water-soluble sodium salt **2** – substituted with a 2-(3-chloro-4-hydroxyphenyl)ethenyl group at the position 3 of the difluoroboradiaza-*s*-indacene core (Fig. 1). The basic structure of *o*-chlorophenol was preserved to obtain the most favorable pK_a value [7]. It is expected that the introduction of a styryl group at the 3-position will lead to a shift of both excitation and emission bands by ~100 nm to the red [14], elevated

* Corresponding author. Tel.: +32 16 327497; fax: +32 16 327990.
E-mail address: Noel.Boens@chem.kuleuven.be (N. Boens).

1010-6030/$ – see front matter © 2006 Elsevier B.V. All rights reserved.
doi:10.1016/j.jphotochem.2006.03.015

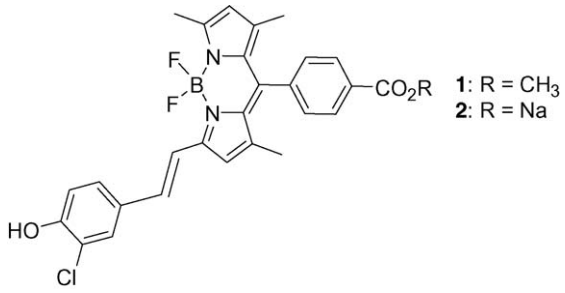

Fig. 1. Chemical structure of *UBphen*: methyl ester **1** and sodium salt **2**.

photostability, high fluorescence quantum yield and absorption coefficients, and a significant absorption wavelength shift upon (de)protonation.

2. Experimental

2.1. Materials

The chemicals for the synthesis were of reagent grade quality, procured from commercial sources, and used as received. All solvents for the spectroscopic measurements were of spectroscopic grade and were used without further purification. Potassium chloride (KCl, 99.999%) and MOPS (3-[*N*-morpholino]propanesulfonic acid, >99.5%) were obtained from Sigma–Aldrich and were used as such.

2.2. Instrumentation

^{1}H and ^{13}C NMR spectra were recorded on instruments operating at a frequency of 300 MHz for ^{1}H and 75 MHz for ^{13}C. ^{1}H NMR spectra were referenced to tetramethylsilane (0.00 ppm) as an internal standard. Chemical shift multiplicities are reported as s = singlet, d = doublet, and m = multiplet. ^{13}C spectra were referenced to the $CDCl_3$ (77.67 ppm) signal. Mass spectra were recorded in E.I. mode. Melting points are uncorrected.

2.3. Steady-state spectroscopy

The absorption measurements were done on a Perkin-Elmer Lambda 40 UV/Vis spectrophotometer. Corrected steady-state excitation and emission spectra were recorded on a SPEX Fluorolog. For the determination of the fluorescence quantum yields (ϕ_f), dilute solutions with an absorbance below 0.1 (1 cm optical path length) at the excitation wavelength λ_{ex} were used. Cresyl violet in methanol ($\lambda_{ex} = 546$ nm, $\phi_f = 0.55$) was used as a fluorescence standard [15]. The ϕ_f values reported in this work are the averages of multiple (generally 4) fully independent measurements. In all cases, correction for the refractive index was applied. All spectra were recorded at room temperature on nondegassed samples.

2.4. Time-resolved spectroscopy

Fluorescence decay traces of compound **1** were recorded by the single-photon timing method [16]. Details of the instrumentation used [17] and experimental procedures [18] have been described elsewhere. The samples were excited at 543 nm with a repetition rate of 4.09 MHz, yielding fluorescence decay histograms in 4096 channels. Using 10 mm × 10 mm cuvettes, fluorescence decays at several emission wavelengths were recorded. The absorbance at the excitation wavelength was always below 0.1. Histograms of the instrument response functions (using LUDOX scatterer), and sample decays were recorded until they typically reached 10^4 counts in the peak channel. The total width at half maximum of the instrument response function was ~60 ps. All fluorescence decays were recorded at 20 °C using nondegassed samples.

The fitting parameters were determined by nonlinear least-squares by minimizing the global reduced chi-square χ^2_g:

$$\chi^2_g = \sum_l^q \sum_i \frac{w_{li}(y^o_{li} - y^c_{li})^2}{\nu} \quad (1)$$

where the index l sums over q experiments, and the index i sums over the appropriate channel limits for each individual experiment. y^o_{li} and y^c_{li} denote respectively the observed and calculated (fitted) values corresponding to the ith channel of the lth experiment, and w_{li} is the corresponding statistical weight. ν represents the number of degrees of freedom for the entire multidimensional fluorescence decay surface.

The additional statistical criteria to judge the quality of the fit have been described elsewhere [19]. The decays were analyzed first individually in terms of decay times τ_i and their associated preexponential factors α_i. The final curve-fitting was done by global analysis in which decays recorded at four different emission wavelengths λ_{em} (from 570 to 630 nm in steps of 20 nm) were described by a monoexponential decay function with a linked lifetime τ and local preexponentials α. The goodness-of-fit was judged for each fluorescence decay trace separately as well as for the global fluorescence decay surface. All curve fittings presented here had χ^2 values below 1.1.

2.5. Determination of K_a from direct fluorimetric titration

The expression of the steady-state fluorescence signal F as a function of the ion concentration has been derived by Kowalczyk et al. for the case of a 1:1 complex between a fluorescent indicator and an analyte (here H^+) [20]. The expression has been extended to the case of a n:1 complex between cation and indicator (Eq. (2)) [21]. The K_a values of the fluorescent pH indicator **2** were determined by fluorimetric titration as a function of pH using the fluorescence excitation or emission spectra (at least four independent measurements were used to compute the average K_a value). Nonlinear fitting of Eq. (2) to the steady-state fluorescence data F recorded as a function of $[H^+]$ yields values of K_a, the fluorescence signals F_{min} and F_{max} at minimal and maximal $[H^+]$, respectively (corresponding to the basic and acid forms of the pH probe, respectively), and n (the number of protons bound per fluorescent pH probe). Eq. (2) assumes that the absorbance of the sample is small (<0.1) and that the binding of

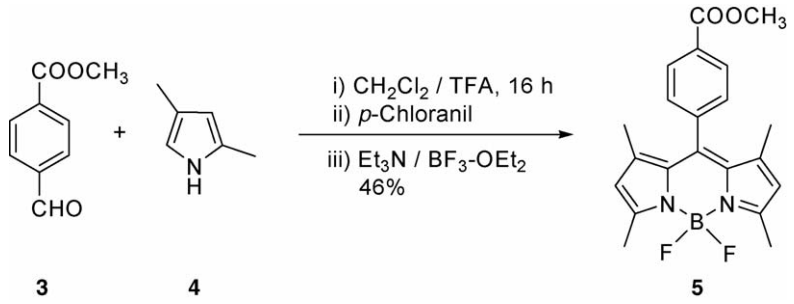

Scheme 1.

H^+ to the probe in the excited state is negligible:

$$F = \frac{F_{max}[H^+]^n + F_{min}K_a}{K_a + [H^+]^n} \quad (2)$$

Fitting Eq. (2) to the steady-state fluorescence data F with n, K_a, F_{min}, and F_{max} as freely adjustable parameters always gave values of n close to 1, indicating that one proton is bound per indicator molecule. Therefore, n was kept fixed at 1 in the final curve fittings, from which the estimated values of K_a are reported here (Tables 2 and 3).

2.6. Determination of K_a from ratiometric absorption titration

Since large spectral shifts are observed in the absorption spectra of **2**, the *ratiometric* method can be used to estimate the ground-state acidity constant K_a (Eq. (3)):

$$R = \frac{R_{max}[H^+]^n + R_{min}K_a\xi}{K_a\xi + [H^+]^n} \quad (3)$$

$R = A(\lambda^1_{abs})/(\lambda^2_{abs})$ is the ratio of the absorbances at the two indicated wavelengths. Nonlinear fitting of Eq. (3) to the absorption ratiometric data R recorded as a function of $[H^+]$ yields values of $K_a\xi$, the ratios R_{min} and R_{max} at minimal and maximal $[H^+]$, respectively (corresponding to the basic and acid forms of the pH probe, respectively), and n (the number of protons bound per pH probe). Since $\xi = A_{min}(\lambda^2_{abs})/A_{max}(\lambda^2_{abs})$ – the ratio of the absorbances at the indicated wavelength – is experimentally accessible, a value for K_a can be extracted from ratiometric absorption data. Note that $\xi = 1$ if the wavelength corresponding to the isosbestic point is taken as λ^2_{abs}.

2.7. Synthesis

4,4-Difluoro-8-[4-(methoxycarbonyl)phenyl]-1,3,5,7-tetramethyl-3a,4a-diaza-4-bora-*s*-indacene (**5**) (Scheme 1).

492 mg (3 mmol) of methyl 4-formylbenzoate (**3**) and 570 mg (6 mmol) of 2,4-dimethylpyrrole (**4**) were dissolved in 50 mL of dry dichloromethane. One drop of trifluoroacetic acid (TFA) was added to the solution and the reaction mixture was stirred for 16 h at room temperature under argon atmosphere. After disappearance of the aldehyde (monitored via thin-layer chromatography), a solution of 500 mg of *p*-chloranil in dichloromethane (30 mL) was added and stirring was continued for another 0.5 h. 3 mL of absolute triethylamine was then added to the mixture and after stirring for 15 min, 3 mL of BF_3-OEt_2 was added dropwise. The stirring was continued for the next 2 h and then the mixture was washed with water and extracted with dichloromethane (3× 50 mL). The separated organic phase was dried ($MgSO_4$), concentrated under vacuum, and purified through a silica column using ethylacetate-hexane 1/4 (v/v) mixture as eluent to obtain 527 mg (46% yield) of shiny brick-red crystals of compound **5**. mp 194–196 °C.

^{1}H NMR (300 MHz, $CDCl_3$) δ 8.20 (d, 2H, J = 8.2 Hz, ArH); 7.43 (d, 2H, J = 8.2 Hz, ArH); 6.00 (s, 2H, H2 and H6); 3.98 (s, 3H, $COOCH_3$); 2.57 (s, 6H, CH_3); 1.37 (s, 6H, CH_3). ^{13}C (75 MHz, $CDCl_3$) δ 15.0, 15.1, 52.9, 122.1, 129.0, 130.9, 131.4, 131.5, 140.4, 140.8, 143.4, 156.6, 167.0; LRMS: (EI, 70 eV) 382

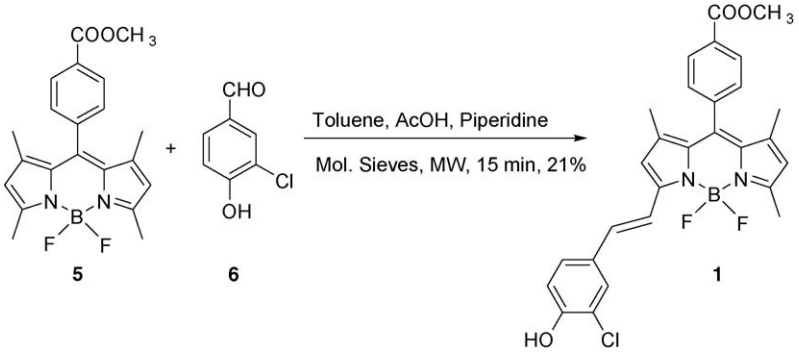

Scheme 2.

(M^+ 100). HRMS (EI) calcd. for $C_{21}H_{21}BF_2N_2O_2$ 382.1664, found 382.1670.

3-[2-(3-Chloro-4-hydroxyphenyl)ethenyl]-4,4-difluoro-8-[4-(methoxycarbonyl)phenyl]-1,5,7-trimethyl-3a,4a-diaza-4-bora-*s*-indacene (**1**) (Scheme 2).

Compound **5** (80 mg, 0.21 mmol), 3-chloro-4-hydroxybenzaldehyde (**6**) (45 mg, 0.29 mmol), piperidine (0.1 mL), acetic acid (0.1 mL) and a small amount of molecular sieves were suspended in 2 mL of dry toluene in a 10 mL glass tube sealed with a teflon cap. The sample was irradiated at 200 W and 190 °C for 20 min in a CEM-Discover monomode microwave apparatus. After completion of the reaction, the cooled mixture was poured directly onto a silica column and eluted with a 1/1 (v/v) dichloromethane/hexane mixture. The collected purple fraction was subsequently recrystallized from chloroform/hexane to yield 23 mg (21% yield) of purple crystals of **1**. mp 135–137 °C.

^{1}H NMR (300 MHz, $CDCl_3$) 8.22 (d, 2H, $J = 8.2$ Hz, aromatic), 7.59–7.50 (m, 3H, aromatic), 7.46 (d, 3H, $J = 8.3$ Hz, aromatic and vinylic), 7.05 (d, 1H, $J = 8.7$ Hz, vinylic), 6.58 (s, 1H, pyrrole), 6.04 (s, 1H, pyrrole), 5.70 (broad singlet, 1H, OH); 3.99 (s, 3H, $COOCH_3$), 1.42 (s, 3H, CH_3), 1.39 (s, 3H, CH_3), 2.62 (s, 3H, CH_3). LRMS (EI, 70 eV) 520 (M^+ 100). HRMS (EI) calcd. for $C_{28}H_{24}BClF_2N_2O_3$ 520.1536, found 520.1530.

3. Results and discussion

Compound **1** (Fig. 1) was synthesized in 21% yield by microwave-assisted condensation of difluoroboradiaza-*s*-indacene derivative **5** with 3-chloro-4-hydroxybenzaldehyde (**6**) using acetic acid–piperidine as a catalyst. The starting compound **5** was synthesized from methyl 4-formyl benzoate (**3**) and 2,4-dimethylpyrrole (**4**) following a literature procedure [22].

3.1. Solvent-dependent spectroscopic properties

The ester form **1** of *UBphen* was dissolved in several solvents to investigate its spectroscopic properties (Table 1). The UV/Vis absorption and fluorescence spectra of 1 in different solvents are depicted in Fig. 2. In all solvents studied, the maximum of the $S_0 - S_1$ absorption band is located between 564 and 576 nm and a shoulder at the short wavelength side (at about 530 nm). The absorption spectra are hardly affected by solvent polarity; the maximum being slightly shifted hypsochromically when the solvent is changed from dimethyl sulfoxide (DMSO, 576 nm) to acetonitrile (564 nm), which is consistent with the general behavior of BODIPY chromophores [4,7,23,24]. Additionally, a broad absorption band is found at about 330 nm, the position of which is not appreciably affected by solvent polarity. This broader absorption band is attributed to the $S_0 - S_2$ transition. The narrow full width at half maximum ($fwhm_{abs}$) of the $S_0 - S_1$ band is typical for BODIPY derivatives [4,7,23,24].

The fluorescence emission spectra (Fig. 2b) display a slightly Stokes-shifted, mirror-symmetrical band typical for borondipyrromethene [4,7,23,24] and the maximum emission wavelength is in the 577–595 nm range. The solvent indepen-

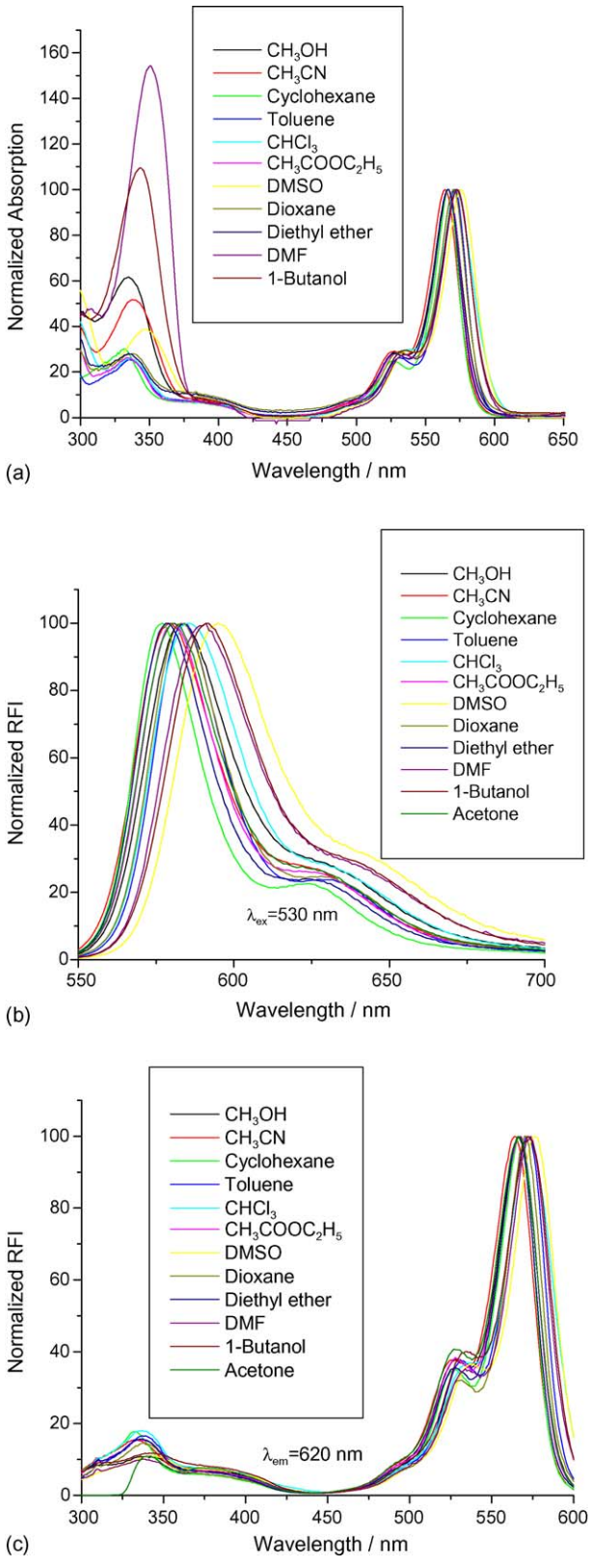

Fig. 2. (a) Absorption spectra of **1** in different solvents. (b) Corresponding fluorescence emission spectra ($\lambda_{ex} = 530$ nm) and (c) fluorescence excitation spectra ($\lambda_{em} = 620$ nm).

Table 1
Absorption and fluorescence properties of **1** in different solvents

Solvent	λ_{abs} (max/nm)	λ_{em} (max/nm)	$\Delta\bar{\nu}$[a] (cm^{-1})	$fwhm_{abs}$[b] (cm^{-1})	ϕ_f[c]	τ[d] (ns)	k_f[e] ($\times 10^8$ s^{-1})
Cyclohexane	567	577	306	659	0.98 ± 0.01	3.53	2.8
1,4-Dioxane	570	583	391	742	0.98 ± 0.01	3.96	2.5
Toluene	571	584	390	709	1.00 ± 0.04	3.58	2.8
Diethyl ether	566	579	397	752	0.98 ± 0.01	4.20	2.3
Chloroform	572	585	389	950	1.00 ± 0.01	3.82	2.6
Ethyl acetate	567	580	395	752	0.99 ± 0.02	3.86	2.6
1-Butanol	573	591	532	827	0.93 ± 0.05	3.79	2.5
Acetone	567	581	425	752	1.00 ± 0.09	4.21	2.4
Methanol	567	584	513	848	0.98 ± 0.04	3.86	2.5
Acetonitrile	564	580	489	791	1.00 ± 0.03	3.95	2.5
DMF[f]	573	591	532	795	1.00 ± 0.05	3.60	2.8
DMSO[g]	576	595	554	819	1.00 ± 0.04	3.58	2.8

[a] Stokes shift.
[b] Full width at half maximum of the $S_0 - S_1$ absorption band.
[c] Fluorescence quantum yield.
[d] The standard errors on all lifetimes τ are $\leq$10 ps.
[e] The rate constant for radiative (k_f) deactivation is calculated from the measured ϕ_f and τ according to $k_f = \phi_f/\tau$.
[f] *N*,*N*-dimethylformamide.
[g] Dimethyl sulfoxide.

dence of the Stokes shift indicates that there is no appreciable change between the dipole moments of ground and excited states. The fluorescence excitation spectra (Fig. 2c) closely match the absorption spectra. The fluorescence quantum yields ϕ_f for **1** are (close to) 1.0 in all solvents studied.

To investigate the fluorescence dynamics of **1**, fluorescence decay traces in different solvents were collected as a function of emission wavelength λ_{em}. The results of the time-resolved fluorescence experiments are also shown in Table 1. The lifetimes τ estimated via single curve analysis were independent of the observation wavelength λ_{em}. Simultaneous (global) curve-fitting of the fluorescence decay surface with τ linked as a function of λ_{em} confirmed that the decays are monoexponential and do not depend on λ_{em}. In all solvents used, a single decay component on the nanosecond timescale with an almost identical lifetime (3.8 ± 0.2 ns) was found. This indicates that the fluorescence properties of *UBphen* are nearly independent of the polarizability and polarity of the solvents. The values of k_f, calculated using the globally estimated τ values and quantum yields ϕ_f, are shown to be independent of the solvent used [$k_f = (2.6 \pm 0.2) \times 10^8$ s^{-1}, Table 1]. Since the fluorescence quantum yields ϕ_f for **1** are (nearly) 1.0 in all solvents studied, the excited-state deactivation occurs almost exclusively through emission.

3.2. pH dependence of the absorption and fluorescence spectra

To study the protonation–deprotonation properties of *UBphen* in aqueous solution, methyl ester **1** was saponified as previously described [25] to yield the corresponding sodium salt **2**. The absorption spectra of **2** as a function of pH in water solution (Fig. 3a) show a decrease of the absorbance band at 590 nm with increasing H^+ concentration (lower pH) and a simultaneous increase of the absorption at 558 nm. Varying the pH also gives rise to an isosbestic point at 570 nm. The lowest-energy absorption band of the phenolic (that is, acidic) form of dye **2** is blue-shifted by about 32 nm in comparison with that of the phenolate ion. Hence, compound **2** shows a chromogenic behavior in the near-neutral pH range by changing the color of the aqueous solution from bright red at low pH to blue at high pH, which can be detected with the naked eye. The pK_a of **2** and the stoichiometry of the proton binding by the phenoxide anion were determined by the changes of the absorbance as a function of pH. The results obtained at λ_{abs} = 590 nm indicated a 1:1 stoichiometry and yielded a value of 7.61 ± 0.06 for pK_a. Since there is a large shift of the absorption spectra, ratiometric absorption measurements could be performed. A pK_a value of 7.54 ± 0.07 was determined by using the ratio of the decrease/increase in the absorption bands at $\lambda^1_{abs}/\lambda^2_{abs}$ = 590/558 nm. If the wavelength of the isosbestic point was chosen as second wavelength (λ^2_{abs} = 570 nm), the pK_a values estimated from ratiometric absorption measurements at λ^1_{abs} = 558 and 590 nm were 7.49 ± 0.06 and 7.56 ± 0.05, respectively. Fig. 4a shows the best fit of Eq. (3) with n = 1 to the *ratiometric* absorption (from Fig. 3a) titration data of **2** ($\lambda^1_{abs}/\lambda^2_{abs}$ = 590/558 nm).

The fluorescence emission spectra of **2** are shown as a function of pH in Fig. 3b. The fluorescence signals increase considerably at lower pH. In contrast to the absorption spectra, the fluorescence emission maximum at 574 nm remains unchanged while the intensity increases with decreasing pH. At all pH values the fluorescence emission spectra resemble those of compound **1** in different solvents, implying that the fluorescence originates solely from the excited phenolic form of **2**. The highest ϕ_f value (0.75) is found at pH ~ 6.50. The excited phenoxide form of **2** in water is non-emissive due to a very efficient ICT process in the excited state from the oxygen atom of the phenoxide ion to the borondipyrromethene moiety. The fact that the phenoxide form of the excited probe **2** is not fluorescent explains

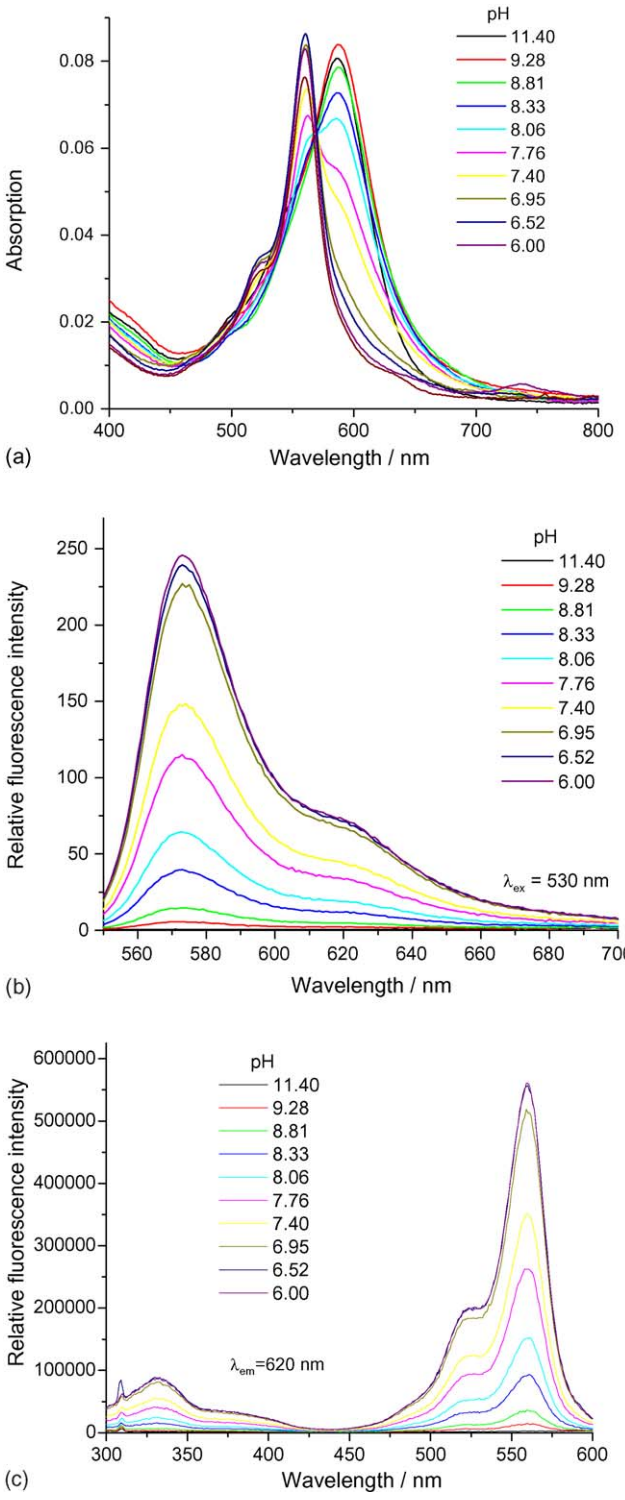

Fig. 3. (a) Absorption spectra, (b) fluorescence emission spectra (λ_{ex} = 530 nm) and (c) fluorescence excitation spectra (λ_{em} = 620 nm) of **2** in aqueous non-buffered solutions as a function of pH.

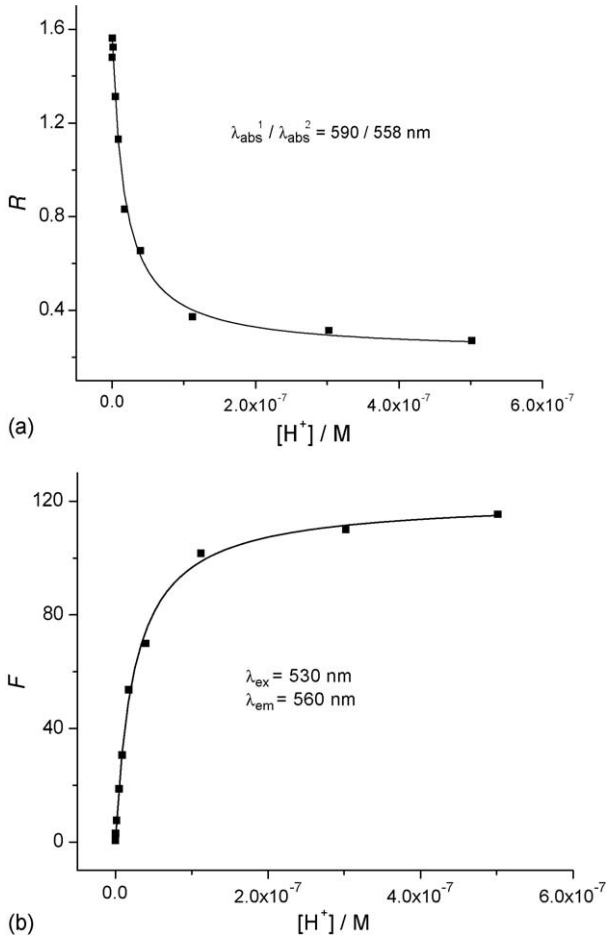

Fig. 4. (a) The solid line represents the best fit of Eq. (3) with $n = 1$ to the *ratiometric* absorption (from Fig. 3a) titration data of **2** ($\lambda^1_{abs}/\lambda^2_{abs}$ = 590/558 nm). (b) Best fit of Eq. (2) with $n = 1$ to the *direct* fluorimetric emission titration data (from Fig. 3b) of 2 (λ_{ex} = 530 nm and λ_{em} = 560 nm) as a function of [H$^+$].

the absence of pH dependent shifts of the fluorescence emission bands. Binding of H$^+$ by the phenoxide ion raises the energy of the ICT state and hence suppresses the formation of this state. Protonation blocks this non-radiative decay channel and leads to a large fluorescence enhancement. The difference between the absorption and excitation spectra (see Fig. 3c) points to the presence of two different species (phenolic and phenolate) in aqueous medium in the near-neutral pH range. The average pK_a value (7.60 ± 0.05) obtained from *direct* fluorimetric titrations using excitation or emission spectra are in excellent agreement with those from (*ratiometric*) absorption measurements. Fig. 4b shows the best fit of Eq. (2) with $n = 1$ to the *direct* fluorimetric (from Fig. 3b) emission titration data of **2** (λ_{ex} = 530 nm and λ_{em} = 560 nm) as a function of [H$^+$]. The K_a values of **2** determined by nonlinear curve-fitting using Eqs. (2) and (3) are compiled in Table 2.

3.3. Effect of ionic strength on K_a

To study the influence of buffer and added salt on the steady-state fluorescence, we recorded pH dependent fluorescence emission and excitation spectra of **2** under various conditions of added MOPS buffer and KCl at 20 °C. The estimated pK_a values are given in Table 3, indicating that K_a of **2** is nearly insensitive to added salt and/or MOPS buffer in the concentration range studied. As the effects of added salt and buffer on the

Table 2
Titration data for **2** determined in water solution in the absence of buffer and salt

Method	Experimental conditions	Ratio	pK_a
Abs	$\lambda_{abs} = 590$ nm	0.25 (A_{max}/A_{min})	7.61 ± 0.06
	$\lambda_{abs} = 558$ nm	1.68 (A_{max}/A_{min})	7.5 ± 0.1
	$\lambda^1_{abs}/\lambda^2_{abs} = 590/558$ nm	0.14 (R_{max}/R_{min})	7.54 ± 0.07
	$\lambda^1_{abs}/\lambda^2_{abs} = 558/590$ nm	6.79 (R_{max}/R_{min})	7.60 ± 0.07
	$\lambda^1_{abs}/\lambda^2_{abs} = 590/570$ nm	0.26 (R_{max}/R_{min})	7.56 ± 0.05
	$\lambda^1_{abs}/\lambda^2_{abs} = 558/570$ nm	1.78 (R_{max}/R_{min})	7.49 ± 0.06
Ex	$\lambda_{em} = 620$ nm, $\lambda_{ex} = 550$ nm	417 (F_{max}/F_{min})	7.60 ± 0.05
	$\lambda_{em} = 620$ nm, $\lambda_{ex} = 560$ nm	685 (F_{max}/F_{min})	7.60 ± 0.03
Em	$\lambda_{ex} = 530$ nm, $\lambda_{em} = 560$ nm	218 (F_{max}/F_{min})	7.60 ± 0.04
	$\lambda_{ex} = 530$ nm, $\lambda_{em} = 570$ nm	240 (F_{max}/F_{min})	7.60 ± 0.04

Table 3
pK_a values of **2** determined by *direct* fluorimetric titration and *ratiometric* absorption titration in the absence/presence of MOPS buffer and added KCl

Experimental conditions	pK_a
0 M MOPS + 0 M KCl	7.60 ± 0.05
0.01 M MOPS + 0 M KCl	7.57 ± 0.01
0.05 M MOPS + 0 M KCl	7.62 ± 0.02
0 M MOPS + 0.1 M KCl	7.59 ± 0.04
0.05 M MOPS + 0.1 M KCl	7.46 ± 0.06

K_a value of **2** are very small, *UBphen* has the advantage of a negligible sensitivity to low ionic strength.

4. Conclusion

A novel borondipyrromethene-derived pH indicator (available as methyl ester (**1**) and sodium salt (**2**)) for the near-neutral pH range with ultra bright fluorescence in the red spectral region has been synthesized by linking *o*-chlorophenol to the 3-position of difluoroboradiazaindacene. Absorption and steady-state and time-resolved fluorescence measurements have been used to study the photophysical properties of compound **1**. The fluorescence lifetime (3.8 ± 0.2 ns) and the fluorescence rate constant ($k_f = (2.6 \pm 0.2) \times 10^8\ s^{-1}$) of dye 1 are independent of the solvent. In aqueous solution, the water-soluble dye (compound **2**) undergoes a reversible protonation–deprotonation reaction (between phenol and phenoxide) in the near-neutral pH range responsible for the observed spectroscopic changes. The pK_a of 7.60 is practically insensitive to low ionic strength. The very high fluorescence quantum yield of the acidic form (0.75) of **2** in aqueous solution, the capability of using longer excitation/emission wavelengths, and the high fluorescence enhancement factor make the new BODIPY derivative an excellent on/off fluorescent pH probe.

Acknowledgements

The University Research Fund of the K.U. Leuven is thanked for grant IDO/00/001 and postdoctoral fellowships to W.Q. and M.B. The Fonds voor Wetenschappelijk Onderzoek – Vlaanderen is thanked for a postdoctoral fellowship to W.M.D.B.

References

[1] (a) J.-P. Desvergne, A.W. Czarnik (Eds.), Chemosensors of Ion and Molecule Recognition, Kluwer, Dordrecht, 1997;
(b) B. Valeur, Molecular Fluorescence, Wiley–VCH, Weinheim, 2002.
[2] R.P. Haugland, The Handbook. A Guide to Fluorescent Probes and Labeling Technologies, 10th ed., Molecular Probes, Inc., Eugene, 2005, pp. 935–947.
[3] A. Treibs, F.-H. Kreuzer, Liebigs Ann. Chem. 718 (1968) 208–223.
[4] E. Vos de Wael, J.A. Pardoen, J.A. Van Koeveringe, J. Lugtenburg, Recl. Trav. Chim. Pays-Bas. 96 (1977) 306–309.
[5] BODIPY is a Registered Trademark of Molecular Probes, Inc., Eugene, Oregon, USA.
[6] (a) J. Karolin, L.B.-Å. Johansson, L. Ny, T. Strandberg, J. Am. Chem. Soc. 116 (1994) 7801–7806;
(b) M. Kollmannsberger, T. Gareis, S. Heinl, J. Breu, J. Daub, Angew. Chem. Int. Ed. 36 (1997) 1333–1335;
(c) T.G. Pavlopoulos, M. Shah, J.H. Boyer, Appl. Opt. 27 (1998) 4998–4999;
(d) K. Rurack, M. Kollmannsberger, U. Resch-Genger, J. Daub, J. Am. Chem. Soc. 122 (2000) 968–969;
(e) Y. Gabe, Y. Urano, K. Kikuchi, H. Kojima, T. Nagano, J. Am. Chem. Soc. 126 (2004) 3357–3367.
[7] (a) M. Baruah, W. Qin, N. Basarić, W.M. De Borggraeve, N. Boens, J. Org. Chem. 70 (2005) 4152–4157;
(b) W. Qin, M. Baruah, A. Stefan, M. Van der Auweraer, N. Boens, ChemPhysChem. 6 (2005) 2343–2351.
[8] K. Yamada, Y. Nomura, D. Citterio, N. Iwasawa, K. Suzuki, J. Am. Chem. Soc. 127 (2005) 6956–6957.
[9] (a) J.-P. Malval, I. Leray, B. Valeur, New. J. Chem. 29 (2005) 1089–1094;
(b) M. Baruah, W. Qin, R.A.L. Vallée, D. Beljonne, T. Rohand, W. Dehaen, N. Boens, Org. Lett. 7 (2005) 4377–4380.
[10] A. Coskun, E.U. Akkaya, J. Am. Chem. Soc. 127 (2005) 10464–10465.
[11] Y. Wu, X. Peng, B. Guo, J. Fan, A. Zhang, J. Wang, A. Cui, Y. Gao, Org. Biomol. Chem. 3 (2005) 1387–1392.
[12] T. Gareis, C. Huber, O.S. Wolfbeis, J. Daub, Chem. Commun. (1997) 1717–1718.
[13] C.N. Baki, E.U. Akkaya, J. Org. Chem. 66 (2001) 1512–1513.
[14] (a) K. Rurack, M. Kollmannsberger, J. Daub, New. J. Chem. 25 (2001) 289–292;
(b) K. Rurack, M. Kollmannsberger, J. Daub, Angew. Chem. Int. Ed. 40 (2001) 385–387.
[15] J. Olmsted, J. Phys. Chem. 83 (1979) 2581–2584.
[16] (a) D.V. O'Connor, D. Phillips, Time-correlated Single Photon Counting, Academic Press, New York, 1984;
(b) N. Boens, in: W.R.G. Baeyens, D. De Keukeleire, K. Korkidis (Eds.), Luminescence Techniques in Chemical and Biochemical Analysis, Marcel Dekker, New York, 1991, pp. 21–45.
[17] M. Maus, E. Rousseau, M. Cotlet, G. Schweitzer, J. Hofkens, M. Van der Auweraer, F.C. De Schryver, A. Krueger, Rev. Sci. Instrum. 72 (2001) 36–40.
[18] L. Crovetto, A. Orte, E.M. Talavera, J.M. Alvarez-Pez, M. Cotlet, J. Thielemans, F.C. De Schryver, N. Boens, J. Phys. Chem. B 108 (2004) 6082–6092.
[19] M. Van den Zegel, N. Boens, D. Daems, F.C. De Schryver, Chem. Phys. 101 (1986) 311–335.
[20] A. Kowalczyk, N. Boens, V. Van den Bergh, F.C. De Schryver, J. Phys. Chem. 98 (1994) 8585–8590.

[21] E. Cielen, A. Tahri, A. Ver Heyen, G.J. Hoornaert, F.C. De Schryver, N. Boens, J. Chem. Soc., Perkin Trans. 2 (1998) 1573–1580.
[22] S.Y. Moon, N.R. Cha, Y.H. Kim, S.-K. Chang, J. Org. Chem. 69 (2004) 181–183.
[23] W. Qin, M. Baruah, M. Van der Auweraer, F.C. De Schryver, N. Boens, J. Phys. Chem. A 109 (2005) 7371–7384.
[24] A. Costela, I. García-Moreno, C. Gomez, R. Sastre, F. Amat-Guerri, M. Liras, F. López Arbeloa, J. Bañuelos Prieto, I. López Arbeloa, J. Phys. Chem. A 106 (2002) 7736–7742.
[25] N. Basarić, M. Baruah, W. Qin, B. Metten, M. Smet, W. Dehaen, N. Boens, Org. Biomol. Chem. 3 (2005) 2755–2761.